Research Article

ADSORPTION KINETIC, EQUILIBRIUM AND THERMODYNAMIC STUDIES ON THE REMOVAL OF MALACHITE GREEN DYE BY ACTIVATED BORASSUS *FLABELLIFER* BARK NANO CARBON

Thiruchelvi M[1]., Senthamilselvi M.M[2]., Venkatraman B.R[3]., Arivoli S[4] and Muruganantham N[5*]

[1]Department of Science, Nagammai Teacher Training Institute, Periyar Centenary Educational Complex, Tiruchirappalli, TamilNadu. India
[2]Office of the Regional Joint Directorate of Collegiate Education, Tiruchirappalli, TamilNadu. India
[3]Post Graduate and Research Department of Chemistry, Periyar E.V.R.College (Autonomous), Tiruchirappalli, TamilNadu. India
[4]Department of Chemistry, Thiru.Vi.Ka. Government Arts College Thiruvarur, Tamil Nadu, India
[5]PG & Research Department of Chemistry, Thanthai Hans Roever College (Autonomous), Perambalur, TamilNadu, India

ARTICLE INFO

ABSTRACT

Dyes are one of the most important industrial pollutants, especially in textile industries. Many methods have been proposed in order to remove color from wastewater among which, adsorption is more acceptable due to the ability for its use in the large scale. In this work the activated Borassus *flabellifer* bark nano carbon (ABNC) has been applied for removal of the malachite green dye from aqueous environments. The effect of pH, contact time, initial concentration and amount of adsorbent were studied. In order to investigate the mechanism of the adsorption process, several kinetic models including pseudo-first order, pseudo-second order and intra-particle diffusion were used. In addition, equilibrium data was fitted on to Langmuir, Freundlich, Temkin, Dubinin-Radushkevich, Hurkins-Jura, Halsay, Radlich-Peterson, Jovanovic and BET isotherm models. Results showed that the adsorption of the malachite green was enhanced with increasing initial dye concentration, pH and contact time. The optimum pH was 9. The q_{max} for adsorption of malachite green dye from the Langmuir model was 15.87 mg/g. considering the values of r^2 (0.999) and χ^2, Freundlich isotherm model and pseudo-second order kinetic model had the best fitness. This study has demonstrated that the ABNC with H_2SO_4 can be employed as effective and inexpensive adsorbent for the removal of malachite green from aqueous environments.

INTRODUCTION

Industrial wastewater is considered as one of the major pollutants of the environment [1]. Moreover, textile industries are among each country's basic industries and have coloured wastewater due to making use of coloured materials [2]. Overall, coloured wastewater is produced by various industries, such as textile, dyeing, pharmaceutical, food, cosmetics and healthcare, paper and leather industries. Such colors not only change the water's colour, which is important regarding aesthetics, but they also prevent light from penetrating through water, disturb photosynthesis and destroy the aquatic ecosystem as well as several aquatic species [2, 3]. One of the high consuming materials in the dye industry is Malachite Green (MG) which is used for cotton and silk painting [4].

Corresponding author: **Muruganantham N**
PG & Research Department of Chemistry, Thanthai Hans Roever College (Autonomous), Perambalur, TamilNadu, India

Up to now, a great number of methods have been proposed in order to remove dyes from the industrial wastewater among which adsorption is the most acceptable one, due to its cost effectiveness and its capability to be used in large scales [5]. The methods of colour removal from industrial effluents include biological treatment, coagulation, flotation, adsorption, oxidation and hyper filtration [3, 4, 6, 7]. Among the treatment options, adsorption has been found to be superior to other techniques for water treatment in terms of initial cost, simplicity of design, ease of operation and insensitivity of toxic substances [7]. Different adsorbents have been used for the removal of various materials from aqueous solutions, such as dyes, metal ions and other organic materials including perlite [4, 6-8], bentonite [9], silica gels [10], fly ash [11], lignite [11], peat [12], silica [13], etc.

Among these natural materials, *Activated* Borassus *flabellifer Bark Nano Carbon (ABNC)* which has a low weight and a fine micro-porous structure (up to 90%) and can be found in many regions of southern part of TamilNadu, India. Because of its fine micro-porous structure, a*ctivated* Borassus *flabellifer bark*

nano carbon (ABNC) has a high specific surface area and can float in water owing to its low density. Recently, many researchers have used activated carbon for removal of cadmium [14], disinfection by-products [15], heavy metals [16], sulfur dioxide [17] and azo dyes [2].

Objectives

Due to several advantages of the a*ctivated* Borassus *flabellifer bark nano carbon (ABNC)* and its accessibility in India, the aim of the present work was to investigate its effectiveness for the removal of (MG) at various experimental conditions. Since initial a*ctivated* Borassus *flabellifer* bark nano carbon (ABNC) has some impurity, shows low sorption capacity and is negatively charged [2], the acidic treated *activated* Borassus *flabellifer* bark nano carbon (ABNC) was used in this work. Therefore, the purpose for acidic treatment of *activated* Borassus *flabellifer* bark nano carbon *(ABNC)* was to improve the positive surface charge of adsorbent and its sorption capacity since initial a*ctivated* Borassus *flabellifer* bark nano carbon (ABNC) shows low sorption capacity. The present study aims to use activated Borassus *flabellifer* bark nano carbon (ABNC) for removing (MG) dye from aqueous solutions.

MATERIALS AND METHODS

Instruments and Reagents

Stock solution was prepared by dissolving the required amount of (MG) in double distilled water. The test solutions were prepared by diluting stock solution to the desired concentrations. The concentration of the (MG) was determined at 620 nm. The pH measurements were done using Digital pH meter (Equip-Tronics EQ 614A, India) and adsorption studies were carried out on UV-Vis Double Beam spectrophotometer (Systronics 2203, India). All chemicals including NaOH, HCl and (MG) with the highest available purity and were purchased from Scientific Equipment Company, Tiruchirappalli (Merck). All solutions were stirred on a hotplate and stirrer (JENWAY, model-1000, India).

Preparing the Adsorbent

The natural plant material Borassus *flabellifer* bark used in the present investigations was collected from Muthupet nearby Thiruvarur district. The bark wastes were washed with distilled water several times to remove the dirt and dust and was subsequently dried in a hot air oven at 110^0C. Afterthat, carbonization of the Borassus *flabellifer* bark was carried out by w/v ratio of concentrated sulphuric acid for 24 hours; the primary carbon was activated at 1100^oC for 6 hours under optimized conditions to obtain activated nano carbon. The activated nano carbon was thereafter transferred to room temperature in an inert atmosphere of nitrogen and washed with hot distilled water and 0.5 N hydrocloric and until the pH of the material reached 7.0. The activated nano carbon was also dried in a hot air oven at 110^0C, ground and sieved to obtain the desired particular size (45nm) and stored in desiccators for further use.

Adsorption Study

To study the effect of important parameters like the pH, contact time and initial dye concentration on the adsorptive removal of MG, batch experiments were conducted. For each experimental run, 50 ml of different concentrations of the dye solution (25 - 125 mg/L) was agitated with 0.025 g of the adsorbent at 120 rpm until the equilibrium was achieved. Samples were withdrawn at different time intervals (15, 30, 45 and 60 minutes) and kinetics, isotherm and other parameters of adsorption was determined by analyzing the remaining dye concentration from aqueous solution. In order to evaluate the effect of the initial pH on (MG) adsorption, the equilibrium study was conducted at different pH levels 3, 4, 5, 6, 7, 8 and 9 and other equilibrium studies were continued at the optimum pH 6.5. The pH of the solutions was adjusted by adding 0.01 N aqueous solutions of NaOH and HCl.

The percentage removal of dye was calculated using the following equation [1, 18]:

$$\%(MG)\ Removal = (C_0 - C_t) / C_0 \times 100 \qquad \ldots\ldots\ldots\ldots (1)$$

Where, C_0 (mg/L) and C_t (mg/L) are the initial dye concentration and dye concentration at time t, respectively. When the system reached the equilibrium concentration, the equilibrium adsorption capacity was calculated by using the following equation:

$$q_e = v\ (C_0 - C_e)/w \qquad \ldots\ldots\ldots\ldots\ldots(2)$$

In this equation, q_e (mg/g) represents the rate of the adsorbed dye per mass unit of the adsorbent, C_0 (mg/L) and C_e (mg/L) are initial and equilibrium dye concentrations, respectively, and v (L) and w (g) are the volume of the dye solution and the weight of the adsorbent, respectively.

RESULTS AND DISCUSSION

The Effect of Contact Time on the Removal of (MG) Dye

Generally, diffusion of the adsorbate onto the adsorbent and ultimately the adsorption phenomena on the adsorbent are time consuming processes [24]. The adsorption rate, obtained for (MG) adsorption on ABNC was observed by decreasing of the concentration of (MG) within the adsorption medium with contact time. The time necessary to reach the equilibrium for the removal of the (MG) molecules at different concentrations (25 - 125 mg/L) by ABNC from aqueous solution was established to be about 60 minutes. As Figure 1 shows, at all the used concentrations, as the contact time between the adsorbent and the adsorbate increased, the adsorption rate increased, as well. According to Figure 1, the highest rate of (MG) removal took place during the 15-30 minute interval. In the remaining concentrations, this reduction continued up to 45 minutes with a lower slope. From this time up to 60 minutes, the system was almost constant and did not have much adsorption. At 25 mg/L of (MG), the removal rate varied from 32.6% to 92.3%.The effect of contact time on the removal of MG onto ABNC are shown in table 1. For instance, the adsorbents exhibited three stages, which can be attributed to each linear portion of the figure. The first linear portion was attributed to the diffusion process of (MG) to the adsorbent surfaces [2, 9], hence, was the fastest sorption stage. This result is corroborated by the fractionary-order kinetic model. The second linear portion was attributed to intra-particle diffusion, which was a delayed process. The third stage may be regarded as the diffusion through smaller pores, which is followed by the establishment of the equilibrium [2, 9]. The surface of ABNC may contain a large number of active sites and the solute uptake can be related to the active sites on equilibrium time. The higher sorption rate at the initial period (first 60 minutes) may be due to an increased number of vacant sites

available at the initial stage. As a result there exists increased concentration gradient between adsorbate in solution and adsorbate in adsorbent surface. This increase in the concentration gradients tends to increase in (MG) sorption at the initial stages.
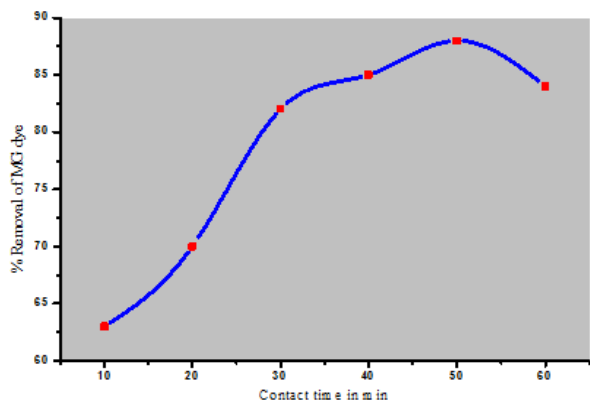

Fig 1 Effect of contact time on the removal of MG dye

The Effect of Initial Concentration of MG on Removal Efficiency

The effect of the initial concentration of MG dye on the adsorption efficiency of the ABNC was evaluated at different concentrations of 25-125 mg/L. In the present study, with the increase of the initial concentration from 25 mg/L to 125 mg/L, the rate of dye removal was reduced from 98% to 93%.The values are shown in table 1. In addition, as the pollutant concentration increased in the aquatic environment, the number of available sites on the adsorbent surface decreased. In other words, with the decrease of the pollutant concentration in the aquatic environment, molecules of the adsorbate have more chance to react with the available active sites on ABNC and, as a result, the adsorption rate is increased. Hence, one could increase the percentage of dye removal by diluting waste water.[25]

Fig 2 Effect of adsorbent dose on the removal of MG dye

The Effect of pH on the Removal Efficiency

pH of the solution affects both aqueous chemistry and surface binding sites of the adsorbents. The effect of initial pH on adsorption of (MG) was studied from pH 2 to 10 at initial (MG) dye concentration of 25 mg/L, adsorbent dosage of 0.025 g and contact time of 60 min. Two possible mechanisms of adsorption of (MG) dye on the ABNC adsorbent may be considered: (a) electrostatic interaction between the adsorbent and the (MG) molecule, (b) a chemical reaction between the (MG) and the adsorbent. When pH increases, the concentration of OH^- ions in the desired solution is increased, as well. This causes the surface of the ABNC to become deprotonated and, as a result, the negative charge of the ABNC surface will be amplified. Therefore, the electrostatic attractive force between the (MG) dye, which has a positive charge, and the adsorbent surface increases, and consequently, the rate of dye adsorption increases, as well [20]. As Figure 3 depicts, as the pH of the solution increased from 2 to 10, the rate of removal also increased up to pH 6.6 then decreased.

Table 1 Equilibrium parameters for the adsorption of MG dye onto ABNC

M_0	C_e (Mg / L)				Q_e (Mg / L)				Removal %			
	30ºC	40ºC	50ºC	60ºC	30ºC	40ºC	50ºC	60ºC	30ºC	40ºC	50ºC	60ºC
25	1.4663	0.8798	0.5872	0.5572	47.068	48.241	48.826	48.886	94.135	96.481	97.651	97.771
50	3.2258	2.9338	2.6516	2.0535	93.549	94.13	94.697	95.893	93.549	94.132	94.697	95.893
75	7.0622	6.3941	5.5718	5.1624	135.88	137.21	138.86	139.68	90.584	91.475	92.571	93.117
100	10.288	9.4088	8.9248	8.3716	179.42	181.18	182.15	183.26	89.712	90.591	91.075	91.628
125	15.249	14.720	14.395	13.540	219.50	220.56	221.21	222.92	87.801	88.224	88.484	89.168

Effect of adsorbent dosage

The adsorption of the MG dye on ABNC was studied by varying the adsorbent dose (25-125 mg/50ml) for 50 mg/L of dye concentration. The percentage of adsorption is increased with increase in the ABNC dose, which is attributed to increased carbon surface area and the availability of more adsorption sites [6,7] Hence, all studies were carried out with 0.025g of adsorbent/50 ml of the varying adsorbate solutions.25, 50, 75, 100 and 125 mg/L. The results obtained from this study are shown in figure 2. The amount of MG dye adsorbed per gram reduced with increase in the dosage of ABNC. This reveals that the direct and equilibrium capacities of MG dye are functions of the activated ABNC dosage.
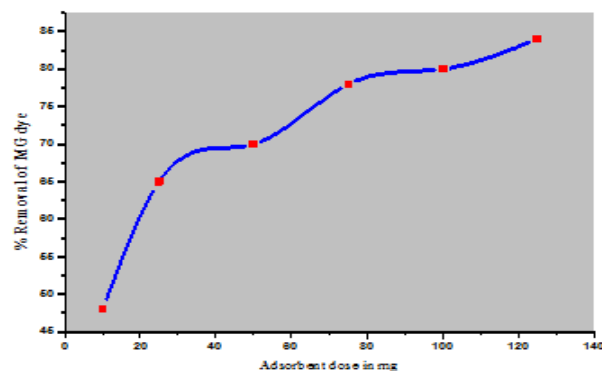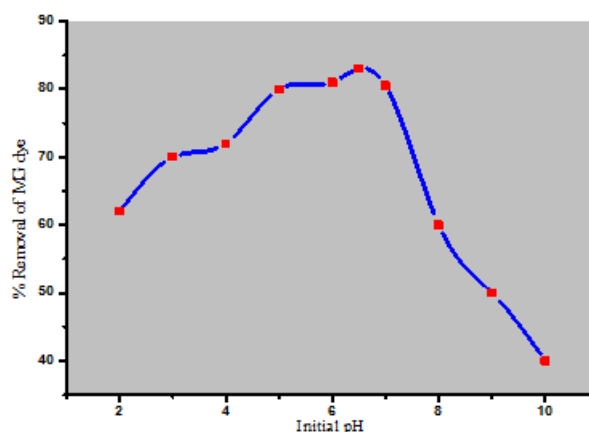

Fig 3 Effect of pH on the removal of MG dye

Adsorption Isotherms

It is important to determine the most appropriate correlation for equilibrium adsorption isotherm, to optimize the design of a sorption system. The Freundlich, Langmuir, Temkin, Hurkins-Jura, Halsay, Redlich-Peterson, Dubinin-Radushkevich, Jovanovich and BET isotherm models were used to analyses the adsorption equilibrium. Experimental isotherm data were obtained at an adsorption time of 60 min at different temperatures.

Freundlich adsorption isotherm

The Freundlich adsorption isotherm is based on the equilibrium sorption on heterogeneous surfaces. This isotherm is derived from the assumption that the adsorption sites are distributed exponentially with respect to heat of adsorption. The adsorption isotherm is expressed by the following equation

$$q_e = K_F C_e^{1/nF} \qquad\qquad\qquad \text{(3)}$$

Which, can be linearized as

$$\ln q_e = \ln K_F + \frac{1}{n_F} \ln C_e \qquad\qquad\qquad \text{(4)}$$

Where, q_e is the amount of MG dye adsorbed at equilibrium (mg/g) and C_e is the concentration of MG dye in the aqueous phase at equilibrium (ppm). K_F (L/g) and $1/n_F$ are the Freundlich constants related to adsorption capacity and sorption intensity, respectively.

The Freundlich constants K_F and $1/n_F$ were calculated from the slope and intercept of the $\ln q_e$ Vs $\ln C_e$ plot. The parameters are shown in Table 2. The magnitude of K_F showed that ABNC had a high capacity for MG dye adsorption from the aqueous solutions studied. The Freundlich exponent, n_F, should have values in the range of 1 and 10 (i.e., $1/n_F < 1$) to be considered as favourable adsorption [23]. $1/n_F$ value of less than 1 indicated that MG dye is favorably adsorbed by ABNC. The Freundlich isotherm did not show a good fit to the experimental data as indicated by SSE and Chi-square statistics.

Langmuir adsorption isotherm

The Langmuir adsorption isotherm is based on the assumption that all sorption sites possess equal affinity to the adsorbate. The Langmuir isotherm in a linear form can be represented as [23]:

$$\frac{C_e}{q_e} = \frac{1}{q_m K_L} + \frac{C_e}{q_m} \qquad\qquad\qquad \text{(5)}$$

Where q_e is the amount of MG dye adsorbed at equilibrium (mg/g), C_e is the concentration of MG in the aqueous phase at equilibrium (ppm), q_m is the maximum MG dye uptake (mg/g), and K_L is the Langmuir constant related to adsorption capacity and the energy of adsorption (g/mg).

A linear plot of C_e/q_e Vs C_e was employed to determine the value of q_m and K_L, the data so obtained are also presented in Table 2. The model predicted a maximum value that could not be reached in the experiments. The value of K_L decreased with an increase in the temperature. A high K_L value indicates a high adsorption affinity. Weber and Chakraborti [24] expressed the Langmuir isotherm in term of dimensionless constant separation factor or equilibrium parameter (R_L) which is defined in the following equation:

$$R_L = \frac{1}{1 + K_L C_0} \qquad\qquad\qquad \text{(6)}$$

Where, C_0 is the initial MG dye concentration (ppm). Four scenarios can be distinguished:

The sorption isotherm is unfavorable when $R_L > 1$, the isotherm is linear when $R_L = 1$, The isotherm is favorable when $0 < R_L < 1$ and the isotherm is irreversible when $R_L = 0$. The values of dimensionless separation factor (R_L) for MG dye removal were calculated at different concentrations and temperatures. As shown in Table 3, at all concentrations and temperatures tested, the values of R_L for MG dye adsorptions on the ABNC were less than 1 and greater than zero, indicating favorable adsorption. The Langmuir isotherm showed a better fit to the adsorption data than the Freundlich isotherm.

Table 2 isotherm parameters for the adsorption of MG dye onto ABNC

Model	Constant	Temperature (°C)			
		30	40	50	60
Freundlich	K_f (mg/g) (L/mg)$^{1/n}$	39.430	51.850	61.770	65.660
	n	1.5541	1.8433	2.0889	2.1076
Langmuir	Q_m (mg/g)	350.21	297.52	275.80	270.95
	b (L/mg)	0.1035	0.1693	0.2333	0.2769
Temkin	b_T (J/mol)	71.616	60.096	53.061	53.384
	K_T (L/mg)	1.423	2.718	3.451	3.758
Hurkins-Jura	A_H (g^2/L)	-2515.0	-2995.5	-3415.2	-3538.9
	B_H (mg^2/L)	-1.0817	-1.0592	-1.0421	-1.0099
Halsay	K_{Ha} (mg/L)	302.0	1448.4	5505.1	6764.2
	n_{Ha}	1.5541	1.8433	2.0889	2.1076
Radlich-Peterson	g	0.3565	0.4575	0.5213	0.5255
	K_R (L/g)	0.0254	0.0193	0.0162	0.0152
Dubinin-Radushkevich	q_s (mg/g)	173.57	163.40	160.39	164.93
	$K_D \times 10^{-4}$ mol^2 kJ^{-2}	1.6405	1.6199	1.6104	1.6154
Jovanovic	K_J (L/g)	0.1015	0.1017	0.1005	0.1045
	q_{max} (mg/g)	55.664	59.678	63.415	65.465
BET	C_{BET} (L/mg)	15.098	27.104	41.582	48.917
	qs (mg/g)	0.0662	0.0369	0.0240	0.0204

The fact that the Langmuir isotherm fits the experimental data well may be due to homogeneous distribution of active sites on the ABNC surface, since the Langmuir equation assumes that the adsorbent surface is energetically homogeneous.

Table 3 Dimensionless seperation factor (r_l) for the adsorption of MG dye onto ABNC

(C_i)	Temperature °C			
	30ºC	40ºC	50ºC	60ºC
25	0.2787	0.1911	0.1464	0.1262
50	0.1619	0.1057	0.0790	0.0674
75	0.1141	0.0730	0.0541	0.0459
100	0.0881	0.0558	0.0411	0.0349
125	0.0717	0.0451	0.0332	0.0281

Temkin adsorption isotherm

The Temkin adsorption isotherm assumes that the heat of adsorption decreases linearly with the sorption coverage due to adsorbent-adsorbate interactions [25.] The Temkin isotherm equation is given as:

$$q_e = \frac{RT}{bT} \ln(K_T C_e) \dots\dots\dots\dots(7)$$

Which, can be represented in the following linear form

$$q_e = \frac{RT}{b} \ln K_T + \frac{RT}{b} \ln C_e \dots\dots\dots\dots(8)$$

Where, K_T (L/g) is the Temkin isotherm constant, b_T (J/mol) is a constant related to heat of sorption, R is the ideal gas constant (8.314 J/mol K), and T is absolute temperature (K). A plot of q_e versus $\ln C_e$ enables the determination of isotherm constants K_T and b_T from the slope and intercept, The parameters are listed in Table 2. The Temkin isotherm appears to provide a good fit to the MG dye adsorption data.

The adsorption energy in the Temkin model, b_T, is positive for MG dye adsorption from the aqueous solution, which indicates that the adsorption is endothermic The experimental equilibrium curve is close to that predicted by Temkin model. Consequently, the adsorption isotherm of MG dye on ABNC can be described reasonably well by the Temkin isotherm.

Hurkins-Jura adsorption isotherm

The Hurkins-Jura adsorption isotherm can be expressed as [26]:

$$q_e = \sqrt{\frac{A_H}{B_H + \log C_e}} \dots\dots\dots\dots(9)$$

This can be rearranged as follows:

$$\frac{1}{q_e^2} = \frac{B_H}{A_H} - \frac{1}{A_H} \log C_e \dots\dots\dots\dots(10)$$

Where, A_H (g^2/L) and B_H (mg^2/L) are two parameters characterizing the sorption equilibrium.

The isotherm equation accounts for multilayer adsorption and can be explained by the existence of a heterogeneous pore distribution. The Harkins-Jura isotherm parameters are obtained from the plots of of $1/q_e^2$ versus log C_e enables the determination of model parameters A_H and B_H from the slope and intercept.

Halsay adsorption isotherm

The Halsay adsorption isotherm can be given as [27]:

$$q_e = \exp\left(\frac{\ln K_{Ha} - \ln C_e}{n_{Ha}}\right) \dots\dots\dots\dots(11)$$

And, a linear form of the isotherm can be expressed as follows:

$$\ln q_e = \frac{\ln K_{Ha}}{n_{Ha}} - \frac{\ln C_e}{n_{Ha}} \dots\dots\dots\dots(12)$$

Where, K_{Ha} (mg/L) and n_{Ha} are the Halsay isotherm constants. A plot of $\ln q_e$ Vs $\ln C_e$, enables the determination of n_{Ha} and K_{Ha} from the slope and intercept. This equation is suitable for multilayer adsorption and the fitting of the experimental data to this equation attest to the heteroporous nature of adsorbent. It also shows that the experimental data and the model predictions are based on the non-linear form of the Halsay models. The model parameters are listed in Table 2. This result also shows that the adsorption of MG dye on ABNC was not based on significant multilayer adsorption. The Halsay model is also not suitable to describe the adsorption of MG dye on ABNC, because this model also assumes a multilayer behavior of the adsorption of adsorbate onto adsorbent.

Radlich-Peterson adsorption isotherm

The Radlich-Peterson adsorption isotherm contains three parameters and incorporates the features of Langmuir and Freundlich isotherms into a single equation. The general isotherm equation can be described as follows [28]:

$$q_e = \frac{K_R C_e}{1 + a_R C_e^g} \dots\dots\dots\dots(13)$$

The linear form of the isotherm can be expressed as follows:

$$\ln \frac{C_e}{q_e} = g \ln C_e - \ln K_R \dots\dots\dots\dots(14)$$

Where, K_R (L/g) and a_R (L/mg) are the Radlich-Peterson isotherm constants and g is the exponent between 0 and 1. There are two limiting cases: Langmuir form for g = 1 and Henry's law for g = 0.

A plot of $\ln C_e/q_e$ versus $\ln C_e$ enables the determination of isotherm constants g and K_R from the slope and intercept. The values of K_R, presented in Table 2, indicate that the adsorption capacity of the ABNC decreased with an increase temperature. Furthermore, the value of g lies between 0 and 1, indicating favorable adsorption.

Dubinin-Radushkevich adsorption isotherm

The Dubinin-Radushkevich adsorption isotherm is another isotherm equation [32]. It is assumed that the characteristic of the sorption curve is related to the porosity of the adsorbent. The linear form of the isotherm can be expressed as follows [29].

$$\ln q_e = \ln Q_D - B_D \left[RT \ln\left(1 + \frac{1}{C_e}\right) \right]^2 \dots\dots\dots\dots(15)$$

Where, Q_D is the maximum sorption capacity (mol/g), and B_D is the Dubinin-Radushkevich constant (mol^2/kJ^2). A plot of $\ln q_e$ Vs $R_T \ln(1 + 1/C_e)$ enables the determination of isotherm constants B_D and Q_D from the slope and intercept, as shown in table 2.

Jovanovic adsorption isotherm

The model of an adsorption surface considered by Jovanovic [30] is essentially the same as that considered by Langmuir. The Jovanovic model leads to the following relationship [29]:

$$q_e = q_{max} \left(1 - e^{K_J C_e} \right)$$

The linear form of the isotherm can be expressed as follows:

$$\ln q_e = \ln q_{max} - K_J C_e$$

Where, K_J (L/g) is a parameter. q_{max} (mg/g) is the maximum MG dye uptake. The q_{max} is obtained from a plot of $\ln q_e$ and C_e, Their related parameters are listed in Table 2.

By comparing the values of the error functions, it was found the Langmuir and Temkin models are best to fit the MG adsorption on the ABNC. Both models show a high degree of correlation. This is clearly confirming the good fit of Langmuir and Temkin models with the experimental data for removal of MG dye from the solution.

The Brunauer-Emmett-Teller (BET) isotherm model

Brunauer-Emmett-Teller (BET) [31] isotherm is a theoretical equation, most widely applied in the gas-solid equilibrium systems. It was developed to derive multilayer adsorption systems with relative pressure ranges from 0.05 Pa to 0.30 Pa corresponding to a monolayer coverage lying between 0.50 Pa and 1.50 Pa. Its extinction model related to liquid-solid interface is exhibited as:

$$q_e = \frac{q_s C_{BET} C_e}{(C_s - C_e)[1 + (C_{BET} - 1)(C_e/C_s)]} \quad \text{...........(16)}$$

Where, CBET, Cs, qs and qe are the BET adsorption isotherm (L/mg), adsorbate monolayer saturation concentration (mg/L), theoretical isotherm saturation capacity (mg/g) and equilibrium adsorption capacity (mg/g), respectively. As C_{BET} and C_{BET} (C_e/C_s) is much greater than 1, the linear form is represented as

$$\frac{C_e}{q(C_s - C_e)} = \frac{1}{q_s C_{BET}} + \left(\frac{C_{BET} - 1}{q_s C_{BET}} \right) \left(\frac{C_e}{C_s} \right) \quad \text{...........(17)}$$

Where, C_e is equilibrium Concentration (mg/l), C_s is adsorbate monolayer saturation concentration (mg/l) and C_{BET} is BET adsorption relating to the energy of surface interaction (l/mg). The results of BET model are also shown in table 2. The obtained result predicts the monolayer coverage of adsorbate and physisorption mechanism.

Adsorption Kinetics

The rate and mechanism of the adsorption process can be elucidated based on kinetic studies. Dye adsorption on solid surface may be explained by two distinct mechanisms: (1) An initial rapid binding of dye molecules on the adsorbent surface; (2) relatively slow intra-particle diffusion. To analyze the adsorption kinetics of the dye, the pseudo-first-order, the pseudo-second-order, and intra-particle diffusion models were applied [38, 39]. Each of these models and their linear modes of the equations are presented in below.

Kinetic Models and Their Linear Forms		
Model	**Nonlinear Form**	**Linear Form**
Pseudo-first-order	$dq_t/dt = k_1(q_e - q_t)$	$\ln (q_e - q_t) = \ln q_e - k_1 t$ ....(18)
Pseudo-second-order	$dq_t/dt = k_2(q_e - q_t)^2$	$t/q_t = 1/k_2 q_e^2 + (1/q_e)t$ ....(19)

Where, q_e and q_t refer to the amount of (MG) dye adsorbed (mg/g) at equilibrium and at any time, t (min), respectively and k_1 (1/min), k_2 (g/mg.min) are the equilibrium rate constants of pseudo-first order and pseudo-second order models, respectively.

Pseudo-first order model is a simple kinetic model, which was proposed by Lagergren [40] during 1898 and is used for the estimation of the surface adsorption reaction rate. The values of $\ln (q_e - q_t)$ were linearly correlated with t. The plot of $\ln (q_e - q_t)$ vs. t should give a linear relationship from which the values of k_1 will be determined from the slope of the plot. In many cases, the first-order equation of Lagergren does not fit well with the entire range of contact time and is generally applicable over the initial stage of the adsorption processes [41]. In the pseudo-second order model [42], the slope and intercept of the t/qt Vs t plot were used to calculate the second-order rate constant, k_2. The values of equilibrium rate constant (k_2) are presented in Table 4. According to Table 4, the value of r^2 (0.999) related to the pseudo-second order model revealed that (MG) dye adsorption followed this model, which is in agreement with the results obtained by Karagoz et al. [23], Hameed et al. [24], and Altenor et al. [37]. Nevertheless, pseudo-first order and pseudo-second order kinetic models cannot identify the mechanism of diffusion of dye into the adsorbent pores.

Simple Elovich Model

The simple Elovich model is expressed in the form,

$$q_t = \alpha + \beta \ln t \quad \text{......... (20)}$$

Where, q_t is the amount adsorbed at time t, α and β are the constants obtained from the experiment and are shown in table 4. A plot of q_t against $\ln t$ gives a linear relationship for the applicability of the simple Elovich kinetic.

Intra-Particle Diffusion Model

The adsorption process on a porous adsorbent is generally a multi-step process. In order to analyse the mechanism of the adsorption of MG dye by ABNC, the experimental data were tested against the intra-particle diffusion model. The adsorption mechanism of the adsorbate on to the adsorbent follows three consecutive steps: mass transfer across the external film of liquid surrounding the particle, adsorption at the surface of pores and the intra-particle diffusion. The slowest of these steps determines the overall rate of the process. The possibility of intraparticle diffusion resistance which could affect the adsorption is explored by using the intra-particle diffusion model given in the equation,

$$q_t = K t^{1/2} + I \quad \text{.........(21)}$$

Where, K is the intra-particle diffusion rate constant and I is the intercept. A plot of q_t against $t^{1/2}$ is drawn to analyse the possibility of intra-particle diffusion as the rate determining step. A two stage adsorption mechanism with first was rapid and second was slow, has been observed from the experimental data. The plot of q_t against $t^{1/2}$ is multi-linear and deviating from the origin, indicating multi-processes have affected the adsorption [18]. Hence, the first portion of the plot indicates the external mass transfer and the second portion is due to intra-particle or pore diffusion. The results are predicted in table 4.

Thermodynamic treatment of the sorption process

In order to study the feasibility of the adsorption process, the thermodynamic parameters such as free energy, enthalpy and

entropy changes can be estimated from the following equations.

$$K_c = C_{Ae}/C_e \qquad \text{......... (22)}$$

$$\Delta G^0 = -RT \ln K_c \qquad \text{.........(23)}$$

$$\text{Log } K_c = \Delta S^0/2.303R - \Delta H^0/2.303RT \qquad \text{......... (24)}$$

Where C_e is the equilibrium concentration in solution in mg/L and C_{Ae} is the equilibrium concentration on the sorbent in mg/L and K_c is the equilibrium constant. The Gibbs free energy (ΔG^0) for the adsorption of (MG) onto biomass at all temperatures was obtained from Eq.23 and are presented in Table 5. The values of ΔH^0 and ΔS^0 were calculated from the slope and intercept of the plot log K_c against 1/T and are also listed in Table 5.

From Table 5 it is clear that the reaction is spontaneous in nature as ΔG^0 values are negative at all the temperatures studied. Again positive ΔH^o value confirms that the sorption is endothermic in nature. The positive value of ΔS^0 reflects the affinities of the adsorbents for the (MG) dye. The positive value of E_a indicates the endothermic nature of the adsorption process which is in accordance with the positive values of ΔH^0. The results as shown in Table 5 indicate that the probability of the MG dye to stick on surface of biomass is very high as $S^* << 1$, these values confirm that, the sorption process is physisorption.

Error Analysis

In the single-component isotherm studies, the optimization procedure requires an error function to be defined in order to

Table 4 The kinetic parameters for the adsorption of MG dye onto ABNC

C_0	Temp °C	Pseudo second order				Elovich model			Intra-particle diffusion		
		q_e	k_2	γ	h	α	β	γ	K_{id}	γ	C
25	30	49.39	0.0055	0.9866	13.53	60.490	0.2449	0.9894	0.0930	0.9961	1.8036
	40	49.52	0.0101	0.9858	24.88	127.18	0.4081	0.9914	0.0529	0.9888	1.8876
	50	49.65	0.0158	0.9886	39.06	220.67	0.6114	0.9954	0.0344	0.9907	1.9267
	60	49.66	0.0168	0.9897	41.36	108.40	0.6443	0.9924	0.0325	0.9897	1.9306
50	30	96.66	0.0038	0.9919	35.80	68.464	0.1708	0.9958	0.0659	0.9944	1.8481
	40	97.08	0.0042	0.9886	39.22	158.38	0.1788	0.9904	0.0624	0.9897	1.8582
	50	97.61	0.0046	0.9912	44.16	412.30	0.1875	0.9924	0.0588	0.9887	1.8693
	60	98.35	0.0050	0.9929	48.77	282.38	0.2069	0.9894	0.0525	0.9907	1.8849
75	30	138.88	0.0038	0.9869	73.31	82.928	0.1702	0.9904	0.0448	0.9947	1.8723
	40	140.87	0.0041	0.9860	82.34	223.02	0.1566	0.9965	0.0481	0.9887	1.8754
	50	143.06	0.0036	0.9852	73.56	154.52	0.1343	0.9951	0.0557	0.9907	1.8673
	60	142.91	0.0050	0.9854	101.47	448.22	0.1582	0.9967	0.0467	0.9887	1.8875
100	30	183.95	0.0038	0.9873	127.42	17.854	0.1161	0.9941	0.0496	0.9928	1.8672
	40	185.67	0.0035	0.9882	121.71	141.82	0.1139	0.9899	0.0502	0.9897	1.8693
	50	186.50	0.0037	0.9903	130.01	264.43	0.1167	0.9930	0.0486	0.9952	1.8748
	60	187.64	0.0037	0.9914	131.15	305.06	0.1168	0.9961	0.0483	0.9908	1.8780
125	30	224.30	0.0023	0.9901	113.55	35.767	0.0991	0.9908	0.0478	0.9910	1.8529
	40	225.50	0.0022	0.9922	112.77	290.12	0.0976	0.9967	0.0483	0.9897	1.8541
	50	225.84	0.0023	0.9869	119.75	103.31	0.1033	0.9954	0.0454	0.9907	1.8608
	60	227.79	0.0022	0.994	112.72	290.01	0.0966	0.9924	0.0483	0.9939	1.8583

In order to support that physical adsorption is the predominant mechanism, the values of activation energy (E_a) and sticking probability (S^*) were calculated from the experimental data. They were calculated by using the modified Arrhenius type equation related to surface coverage (θ) as follows[49]:

$$\theta = \left(1 - \frac{C_e}{C_i}\right) \qquad \text{.............. (25)}$$

$$S^* = (1-\theta)_e \frac{-E_a}{RT} \qquad \text{.............. (26)}$$

The sticking probability, S^*, is a function of the adsorbate/adsorbent system under consideration but must satisfy the condition $0 < S^* < 1$ and is dependent on the temperature of the system. The values of E_a and S^* were calculated from slope and intercept of the plot of $\ln(1-\theta)$ versus 1/T respectively and are listed in Table 5.

Table 5 Thermodynamic parameter for the adsorption of MG dye onto ABNC

(C_0)	ΔG^o				ΔH^o	ΔS^o	E_a	S^*
	30ºC	40ºC	50ºC	60ºC				
25	-6992.5	-8616.6	-10009.9	-10468.2	29.030	119.66	27963.2	8E-07
50	-6736.6	-7222.0	-7740.4	-8722.5	12.793	64.145	12123.4	5E-04
75	-5702.9	-6175.2	-6774.2	-7211.4	9.8422	51.284	9046.67	3E-03
100	-5455.4	-5893.4	-6237.8	-6624.9	6.2202	38.595	5641.86	1E-02
125	-4972.0	-5240.5	-5475.8	-5836.1	3.5743	28.162	3162.62	3E-02

be able to evaluate the fit of the isotherm to the experimental equilibrium data. However, the use of r^2 is limited for solving the linear forms of the isotherm equation, but not the errors in isotherm curves. In this study, a Chi-square test was used. The Chi-square test statistic is basically the sum of the squares of the differences between the experimental data and data obtained by calculation from models, with each squared difference divided by the corresponding data obtained by calculation from models [45]. The equivalent mathematical statement is:

$$X^2 = \Sigma_{i=1}^m (q_{e,exp} - q_{e,calc})^2 / q_{e,exp} \qquad \text{.............(27)}$$

Where, $q_{e,exp}$ is the experimental data of the equilibrium capacity (mg/g), $q_{e,calc}$ is the equilibrium capacity obtained by calculating from the model (mg/g). Therefore, it is necessary to analyze the data set using the Chi-square test to confirm the best-fit isotherm for the adsorption of (MG) on ABNC. Given the values of r^2, and χ^2 in Table 2 it can be concluded that the Freundlich isotherm model has the best goodness of fit among the applied isotherm models

Effect of other ions

The effect of other ion like Cl^- on the adsorption process studied at different concentrations. The ions added to 50 mg/L of MG solutions and the contents were agitated for 60 min at 30ºC. The results are shown in the Fig. 4 which reveals that low concentration of Cl^- does not affect the percentage of

adsorption of MG dye on ABNC, because the interaction of Cl⁻ at available sites of adsorbent through competitive adsorption is not so effective. This is so because ions with smaller hydrated radii decrease the swelling pressure within the sorbent and increase the affinity of the sorbent for such ions [9].
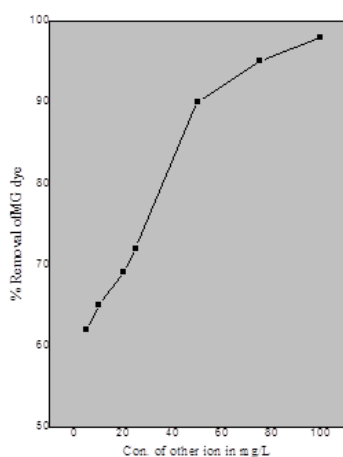

Fig 4 Effect ionic strength on the adsorption of MG dye [MG]=20mg/L; Contact time =60 min; Dose=25mg/50ml

Desorption studies

In order to assess the reusability of MG-loaded ABNC biomass desorption experiments were carried out. The effect of strength of desorbing solution (HCl) on the recovery of MG dye is around 85%. It is evident from the result that when the strength of the desorbing solution increased from 0.5 to 2.0 M, MG desorption percentage increased from 30% to 85%. Thus a significant amount of MG dye is being desorbed, which shows that the ABNC biomass can be effectively reused after desorption [20].

DISCUSSION

The present study investigated the efficiency of ABNC as a cheap adsorbent and the results revealed that ABNC was an appropriate adsorbent for removing (MG) from the aquatic environments. pH also plays a major role in removing the (MG). The findings of the present study also showed that as the contact time increased, the dye's primary concentration as well as the dose of the intended adsorbate of the adsorption efficiency increased, as well. Adsorption equilibrium data follows Langmuir, Freundlich, Temkin and Dubinin-Radushkevich isotherm models. The equilibrium data fitted very well in the Freundlich isotherm equation. The kinetic study of (MG) on to ABNC was performed based on pseudo-first-order, pseudo-second-order and intra-particle diffusion equations. The data indicate that the adsorption kinetics follow the pseudo-second-order rate. This study concludes that the ABNC could be employed as an appropriate, inexpensive, accessible and low-cost adsorbent for the removal of (MG) from aquatic environments.

References

1. Sapci Z, Ustun B. The removal of color and COD from textile wastewater by using waste pumice. *Elec J Environ Agric Food Chem.* 2003; 2(2):286-90.
2. Samarghandi MR, Zarrabi M, Sepehr MN, Amrane A, Safari GH, Bashiri S. Application of acidic treated pumice as an adsorbent for the removal of azo dye from aqueous solutions: kinetic, equilibrium and thermodynamic studies. *Iranian J Environ Health Sci Eng.* 2012;9(1):9.
3. Iqbal MJ, Ashiq MN. Adsorption of dyes from aqueous solutions on activated charcoal. *J Hazard Mater.* 2007;139(1):57-66.
4. Yang J, Qiu K. Preparation of activated carbons from walnut shells via vacuum chemical activation and their application for Malachite Green removal. *Chem Eng J.* 2010;165(1):209-17.
5. Robinson T, McMullan G, Marchant R, Nigam P. Remediation of dyes in textile effluent: a critical review on current treatment technologies with a proposed alternative. *Bioresour Technol.* 2001;77(3):247-55.
6. Santhy K, Selvapathy P. Removal of reactive dyes from wastewater by adsorption on coir pith activated carbon. *Bioresour Technol.* 2006;97(11):1329-36.
7. McKay G, Porter JF, Prasad GR. The removal of dye colours from aqueous solutions by adsorption on low-cost materials. *Water Air Soil Pollut.* 1999; 114(3-4):423-38.
8. Doğan M, Alkan M, Onganer Y. Adsorption of Malachite Green from aqueous solution onto perlite. *Water Air Soil Pollut.* 2000; 120(3-4):229-48.
9. Bereket G, Aro AZ, ozel MZ. Removal of Pb(II), Cd(II), Cu(II), and Zn(II) from Aqueous Solutions by Adsorption on Bentonite. *J Colloid Interface Sci.* 1997; 187(2):338-43.
10. Mohamed MM. Adsorption properties of ionic surfactants on molybdenum-modified silica gels. *Colloids Surf A: Physicochem Eng Aspect.* 1996; 108(1):39-48.
11. Mohan D, Singh KP, Singh G, Kumar K. Removal of dyes from wastewater using flyash, a low-cost adsorbent. *Indust Eng chem Res.* 2002;41(15):3688-95.
12. Ho Y, McKay G. Sorption of dye from aqueous solution by peat. *Chem Eng J.* 1998; 70(2):115-24.
13. McKay G, Otterburn MS, Sweeney AG. Surface mass transfer processes during colour removal from effluent using silica. *Water Res.* 1981;15(3):327-31.
14. Panuccio MR, Sorgona A, Rizzo M, Cacco G. Cadmium adsorption on vermiculite, zeolite and pumice: batch experimental studies. *J Environ Manage.* 2009;90(1):364-74.
15. Kaplan Bekaroglu SS, Yigit NO, Karanfil T, Kitis M. The adsorptive removal of disinfection by-product precursors in a high-SUVA water using iron oxide-coated pumice and volcanic slag particles. *J Hazard Mater.* 2010;183(1-3):389-94.
16. Moraci N, Calabro PS. Heavy metals removal and hydraulic performance in zero-valent iron/pumice permeable reactive barriers. *J Environ Manage.* 2010;91(11):2336-41.
17. Ozturk B, Yildirim Y. Investigation of sorption capacity of pumice for SO 2 capture. Process Safety Environ Protec. 2008;86(1):31-6.
18. Yavuz Ö, Aydin AH. Removal of direct dyes from aqueous solution using various adsorbents. *Polish J Environ Studie*s. 2006; 15(1):155- 61.
19. Alkan M, Doğan M. Adsorption of copper (II) onto perlite. *J Colloid Interface Sci.* 2001; 243(2):280-91.
20. Han R, Wang Y, Han P, Shi J, Yang J, Lu Y. Removal of Malachite Green from aqueous solution by chaff in batch mode. *J Hazard Mater.* 2006; 137(1):550-7.

21. El Qada EN, Allen SJ, Walker GM. Adsorption of methylene blue onto activated carbon produced from steam activated bituminous coal: a study of equilibrium adsorption isotherm. *Chem Eng J.* 2006; 124(1):103-10.

22. Chen H, Zhao J, Dai G. Silkworm exuviae--a new non-conventional and low-cost adsorbent for removal of methylene blue from aqueous solutions. *J Hazard Mater*. 2011; 186(2-3):1320-7.

23. Karagoz S, Tay T, Ucar S, Erdem M. Activated carbons from waste biomass by sulfuric acid activation and their use on methylene blue adsorption. *Bioresour Technol.* 2008; 99(14):6214-22.

24. Hameed BH, Din AT, Ahmad AL. Adsorption of methylene blue onto bamboo-based activated carbon: kinetics and equilibrium studies. *J Hazard Mater.* 2007; 141(3):819-25.

25. Rao GB, Kalyani G, Saradhi BV, Kumar YP. Removal of Fluoride from Aqueous Solution Using a Waste Material. *Nature Environ Pollut Tech*. 2009;8(2):231-6.

26. Langmuir I. The adsorption of gases on plane surfaces of glass, mica and platinum. *J American Chem Soc*. 1918;40(9):1361-403.

27. Abdelwahab O. Evaluation of the use of loofa activated carbons as potential adsorbents for aqueous solutions containing dye. *Desal*. 2008; 222(1):357-67.

28. Ng C, Losso JN, Marshall WE, Rao RM. Freundlich adsorption isotherms of agricultural by-product-based powdered activated carbons in a geosmin-water system. *Bioresour Technol*. 2002; 85(2):131-5.

29. Akbal F. Adsorption of basic dyes from aqueous solution onto pumice powder. *J Colloid Interface Sci.* 2005; 286(2):455-8.

30. Asgari G, Roshani B, Ghanizadeh G. The investigation of kinetic and isotherm of fluoride adsorption onto functionalize pumice stone. *J Hazard Mater*. 2012; 217-218:123-32.

31. Mahvi AH, Heibati B, Mesdaghinia A, Yari AR. Fluoride Adsorption by Pumice from Aqueous Solutions. *J Chem*. 2012; 9(4):1843-53.

32. Veliev EV, Ozturk T, Veli S, Fatullayev AG. Application of diffusion model for adsorption of azo reactive dye on pumice. *Polish J Environ Studies*. 2006; 15(2):347-53.

33. Freundlich H. Über die adsorption in lösungen. Engelmann, Leipzig. 1906; 57(A):385-470.

34. Temkin MJ, Pyzhev V. Recent modifications to Langmuir isotherms. *Acta Physiochim* USSR. 1940; 12:217-22.

35. Dubinin MM, Zaverina ED, Radushkevich LV. Sorption and structure of active carbons. I. Adsorption of organic vapors. Zhurnal Fizicheskoi Khimii. 1947; 21:1351-62.

36. Rieman W, Walton H. Ion Exchange in Analytical Chemistry, International Series of Monographs in Analytical Chemistry. Pergamon Press, Oxford; 1970.

37. Altenor S, Carene B, Emmanuel E, Lambert J, Ehrhardt JJ, Gaspard S. Adsorption studies of Malachite Green and phenol onto vetiver roots activated carbon prepared by chemical activation. *J Hazard Mater*. 2009;165(1-3):1029-39.

38. Çolak F, Atar N, Olgun A. Biosorption of acidic dyes from aqueous solution by Paenibacillus macerans: Kinetic, thermodynamic and equilibrium studies. *Chem Eng J*. 2009;150(1):122-30.

39. Murugan T, Ganapathi A, Valliappan R. Removal of dyes from aqueous solution by adsorption on biomass of mango (Mangifera indica) leaves. *J Chem*. 2010;7(3):669-76.

40. Lagergren S. Zur theorie der sogenannten adsorption geloster stoffe. Kungliga Svenska Vetenskapsakademiens. *Handlingar*. 1898; 24:1-39.

41. Ahmad AA, Hameed BH, Aziz N. Adsorption of direct dye on palm ash: kinetic and equilibrium modeling. *J Hazard Mater*. 2007; 141(1):70-6.

42. Ho Y, McKay G. Pseudo-second order model for sorption processes. *Proc Biochem*. 1999; 34(5):451-65.

43. Weber WJ, Morris JC. Kinetics of adsorption on carbon from solution. *J Sanit Eng Div Am Soc Civ Eng*. 1963; 89(17):31-60.

44. Mall ID, Srivastava VC, Agarwal NK. Removal of Orange-G and Methyl Violet dyes by adsorption onto bagasse fly ash-kinetic study and equilibrium isotherm analyses. *Dyes Pigments*. 2006;69(3):210-23.

45. Amin NK. Removal of direct blue-106 dye from aqueous solution using new activated carbons developed from pomegranate peel: adsorption equilibrium and kinetics. *J Hazard Mater*. 2009; 165(1-3):52-62.

46. S Arivoli, M Hema, S Parthasarathy and N Manju,. Adsorption dynamics of methylene blue by acid activated carbon. *J. Chem. Pharm. Res*, 2010, 2(5), 626-641.

47. M Hema and S Arivoli, Rhodamine B adsorption by activated carbon: Kinetic and equilibrium studies, *Indian Journal of Chemical Technology*, 2009, 16(1), 38-45.

48. V Vijayakumaran, S Arivoli, and S Ramuthai, Adsorption of nickel ion by low cost carbon-kinetic, thermodynamic and equilibrium studies, 2009, 6 (S1), S347-S357.

****